Study of magnetization reversal in hybrid magnets

D. Bueno-Báques, E. Padrón Hernández, J. Matutes-Aquino, S. M. Rezende, D. R. Cornejo

Abstract

A study of magnetic interactions and magnetization reversal at room temperature in hybrid magnets consisting of micrometrics particles of strontium ferrite and Magnequench MQP-Q alloywas carried out. Materials with three different compositions were considered. These materials present different intensity of coupling between their components. In each case, the evolution of the DCD reversible (M_{rev}) and irreversible (M_{irr}) magnetization components during the magnetization and the demagnetization processes was determined. M_{rev} (M_{irr}) Hi curves were built, being Hi the internal field of the sample. In order to investigate the nature of the magnetic interactions between the different grains, a study of the δMd(Hi) plots was developed. The experimental behavior of the $M_{rev}(M_{irr})H$i curves suggest the existence of a complex non-uniform mechanism for the magnetization reversal in these materials. The δM_d(Hi) plots shown a notable predominance of the demagnetizing-like magnetostatic interactions.

Introduction

Bonded magnet is one of the faster growing segments of the permanent magnets market. Bonded magnets are produced by encapsulation of the magnetic powder in a resin or polymer and then compacting or molding the material up to the final shape. Magnetic properties are, in general, inferior to the solid-sintered magnets due to the reduced volume fraction of the permanent magnet material. However, this disadvantage is offset by the very low cost, ease of formability and the improvement in non-magnetic properties such as strength, pliability, elasticity and resistance to fracture. The commercially most used materials for bonded magnets are ferrites and NdFeB. MQP-Q has recently been used with barium ferrite to produce hybrid magnets with interesting coercive properties [1,2]. Barium and strontium ferrites have the unusual property that their coercivities raise with increasing temperature, thus bonded magnets produced by combination of this ferrites and Magnequench alloy MQP-Q (Nd2Fe14B+α-Fe) are very interesting materials due to the coercivity low temperature dependence.

The study of the interactions between the different components in alloys obtained by mixture of different magnetic materials is a very difficult task. However, a graphical interpretation of the interactions can be obtained in terms of the so-called δMd plot, which displays $\delta M_d = m_d - (1–2\ m_r)$ versus the internal field H_i. $m_d = M_d(Hi)/M_R$ and $m_r = M_r(H_i)/M_R$ are the demagnetizing and magnetizing remanences, and MR is the remanence obtained from the saturation [3]. On the δM_d plot, interactions are called “magnetizing” or “demagnetizing” according to whether the experimental points fall above or below the line defined by $\delta M_d(H_i) = 0$.

Recent studies of demagnetization processes in permanent magnets have shown that the behavior of $M_{rev}(M_{irr})H_i$ curves can be used as a mechanism indicator in the magnetization reversal process [4,5]. The dependence between M_{rev} and M_{irr} was expressed by Cammarano et al. [6] as $dM_{rev} = \chi^i_{rev}\ dH_i + \eta\ dM_{irr.}$ η is the interrelation function given by $\eta = (\partial M_{rev}/\partial M_{irr})H_i$, χ^i_{rev} is the reversible susceptibility and Hi is the internal field defined as $H_i = H_{ap} - DM$, where H_{ap} is the applied field and D is the demagnetization factor of the sample. In systems where the magnetization reversal occurs by coherent rotation of non-interacting single domains, linear $M_{rev}(M_{irr})H_i$ curves are expected. If the nucleation and unpinning of inverse domains are the basis of the mechanism in magnetization reversal, the $M_{rev}(M_{irr})H_i$ curves will exhibit a minimum during the demagnetization process [4,5]. This method was previously used to study magnetization reversal in magnetically hard SmCo films [7] and cobalt ferrite powders [8].

In this work, $\delta Md(Hi)$ plots and $M_{rev}(M_{irr})Hi$ curves were used to study the interactions and the reversal magnetization in hybrid magnets of bonded strontium ferrite and MQP-Q alloy.

Experimental

Three isotropic bonded magnets with different composition and densities were considered in this work. Samples were produced by injection molding using commercial MQP-Q (intrinsic coercivity H_c = 3.50 kOe), supplied by Magnequench Int. Inc. and strontium ferrite (intrinsic coercivity H_c = 4.40 kOe), supplied by Hoosier Magnetics Inc. Linear low-density expanded polyethylene (LLDPE) was used as binder. MQP-Q powders have typical particles size of 50μm, with grains of $Nd_2Fe_{14}B$ and α-Fe of 30 nm, approximately. Strontium ferrite has particles size of 50–100 μm. The weight fractions of each magnetic component in each composition were: 48% Sr ferrite + 6% MQP-Q + 46% LLDPE (sample A, density ρA = 1.26 g cm^{-3}), 26% Sr ferrite + 68% MQP-Q + 6% LLDPE (sample B, density ρB = 3.91 g cm^{-3}), 4% Sr ferrite + 82% MQP-Q + 14% LLDPE (sample C, density ρC = 2.86 g cm^{-3}). Sample A is reach in strontium ferrite, but have lower density due to its higher binder content. Samples B and C, on the other hand, are reach in MQP-Q. Long parallelepiped shape samples were cut for magnetic characterization. Measurements of magnetization as a function of applied field were made at room temperature using a vibrating sample magnetometer with a 20 kOe electromagnet. The internal field H_i was calculated using the demagnetization factor appropriate for the geometry of the samples. From the demagnetized state, a set of 39 recoil curves to $H_i = 0$ for progressively increasing positive peak fields was obtained. Afterwards, starting with the sample saturated at 15 kOe, a new set of 39 recoil curves with negative peak fields was measured.

Results and discussion

The saturation magnetization and the coercivity of each sample were determined from the major hysteresis loops: 4πMS = 0.78 kG and Hc = 4.8 kOe (sample A), 4πMS = 6.69 kG and Hc = 4.3 kOe (sample B), 4πMS = 5.41 kG and Hc = 4.4 kOe (sample C). Fig. 1 shows the hysteresis loops of the samples. For comparison, the magnetization was normalized to the respective saturation magnetization. In sample A, the low density of magnetic materials provokes low magnetization and a lower relative remanence, $M_R/M_S = 0.37$. However, its higher coercivity is associated to the better isolation of particles by the binder. On the other hand, samples B and C present normalized hysteresis loops nearly identical, with $M_R/M_S = 0.50$.

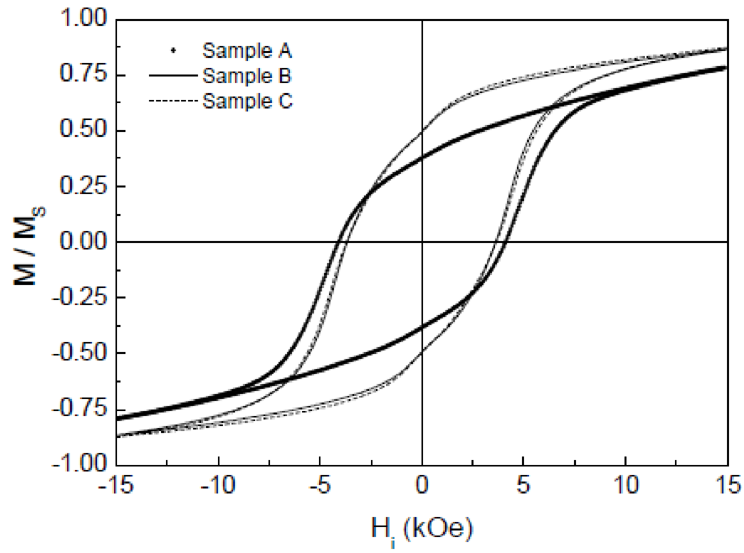

Fig. 1. Major hysteresis loops for each sample of hybrid magnet.

Fig. 2 shows the δM_d plots for the three samples, along with theWohlfarth line $\delta M_d = 0$. For most of the field range, demagnetizing interactions are very strong, especially for samples A and B. This can be due to the high structural disorder of the materials and the intensity of the magnetostatic interactions between grains. Sample C, with higher contents of MQP-Q alloy shows magnetizing interaction between 0 and H_c, reflecting the exchange coupling of the nanograins of α-Fe and $Nd_2Fe_{14}B$.

In these isotropic hybrid magnets, it is possible to guess that the DCD M_{rev} component comes from the initial reversible moving of the domain walls in the grains of strontium ferrite, limited by the pinning centers, and also from a posterior reversible rotation of the magnetic moment of each grain (strontium ferrite) and nanograins (α-Fe and $Nd_2Fe_{14}B$), for higher magnetic fields. When a magnetic field is applied to the initial state (demagnetized or remanence), the system acquires a certain configuration of magnetic moments orientations in every grain. This particular configuration determines the value of M_{irr} . When the field is gradually returned to zero, the magnetic moments in the grains tend to rotate towards its easy magnetization directions. Nevertheless, the pinning centers in strontium ferrite grains, and the exchange coupling between neighboring nanograins of α-Fe and $Nd_2Fe_{14}B$ can prevent the rotation of the complete volume of each grain. Hereby, the initial magnetic state of the sample, the previous value of return magnetic field, the degree of coupling between the grains, and the instantaneous intensity of the internal field determine the behavior of the $M_{rev}(H_i, M_{irr})$ curves.

In Fig. 3, the $M_{rev}(H_i)/M_R$ and $M_{irr}(H_i)/M_R$ curves determined during the initial magnetization process are shown.

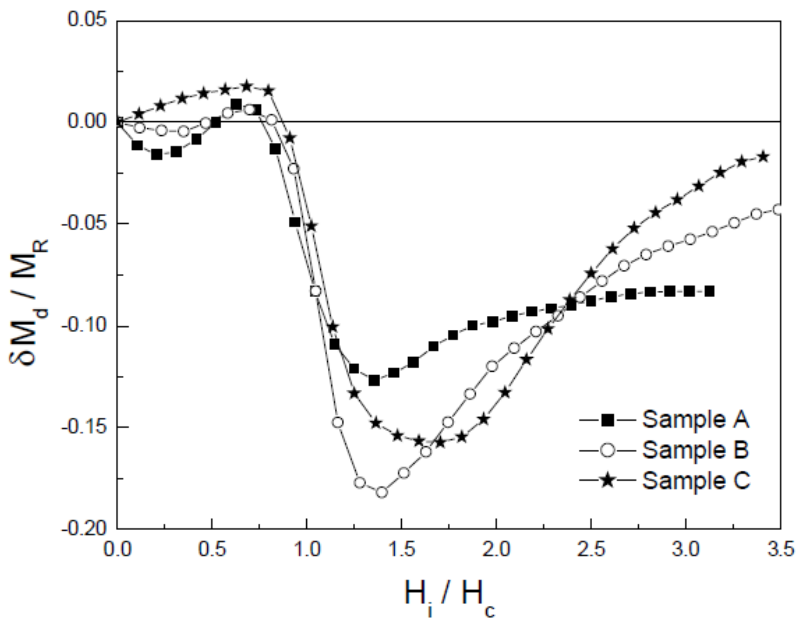

Fig. 2. Magnetic interactions: δM_d values as a function of the reduced internal field for the samples A, B and C.

Also, for direct comparison, the $-M_{rev}(H_i)/M_R$ and $[1 - M_d(H_i)/M_R]/2$ curves [7] from the demagnetization process for each sample are displayed in the same figure. In this last case, $M_d(H_i)/M_R = M_{irr}(H_i)/M_R$ is the demagnetization

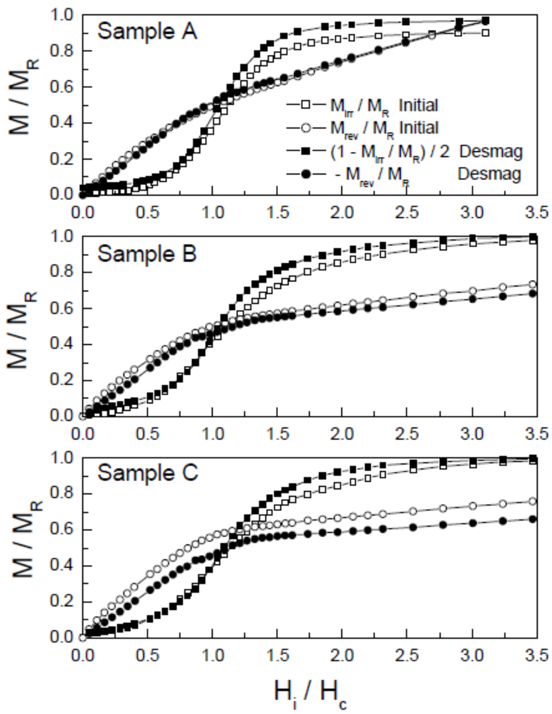

Fig. 3. DCD M_{rev}/M_R ($-M_{rev}/M_R$) and M_{irr}/M_R ($(1 - M_{irr}H_i/M_R)/2$) components as function of the reduced internal field for the initial magnetization (demagnetization) curve for each sample.

remanence normalized by MR. The great quantitative similarity between $M_{irr}(H_i)/M_R$ and $[1 - M_d(H_i)/M_R]/2$ for all samples suggests that the irreversible reversal of the magnetization in the grains, produced by a field H_i, does not depend strongly on magnetic moments initial configuration of directions. For fields higher than H_c, the irreversible component reaches larger values during the demagnetization in comparison with the initial magnetization, because in the remanence state there are more grains aligned antiparalleled to the magnetic field applied later.

All cases initially $|M_{rev}(H_i)/M_R|$ increases faster and remains greater than the corresponding M_{irr} function up to values of internal field close to H_c. In this range of fields, the reversible moving of domain walls and the reversible rotation in the boundary of the grains predominates over the irreversible reversal. Also, in all samples $|M_{rev}|$

shows a decelerating behavior at H_c, probably linked to the establishing of the single domain character in the strontium ferrite grains. The larger magnitude reached by |Mrev| for fields higher than H_c in the sample A can be linked to the ferrite reach composition of the sample and its low density. For fields $H_i > H_c$, relatively big isotropic grains of strontium ferrite can rotate reversibly going the field. When the fraction of ferrite decreases (samples B and C) this contribution to the reversible component also decreases.

Fig. 4 shows representative normalized M_{rev}/M_R versus M_{irr} /M_R curves at different fixed Hi for the demagnetization curve for the three samples. In sample A, two well defined minima at approximately $M_{irr}/M_R = \pm 0.35$ are displaying by the $M_{rev}(M_{irr})H_i$ curves. Crew et al. associated these minima to an increasing of the total domain wall area in the material [4]. In our case, the first minimum can be associated to a fast increase of the total domain wall area, due to the formation of inverse domains in the grains of strontium ferrite and subsequently free displacement of the wall up to a stable position or a pinning site. This minimum is less evident in the samples B and C (poor in ferrite), and then it can be entailed to the strontium ferrite. The second minimum, on the other hand, can be produced by the increasing of the magnetic moments rotation in single domain grains and appears at high internal fields, when M_{irr} is more close to M_R. For the sample C, only this second minimum is clearly obtained indicating that it can be mainly associated to the MQP-Q alloy, which is fully consistent with behaviors shown by isotropic sintered and isotropic melt quenched NdFeB alloys [4].

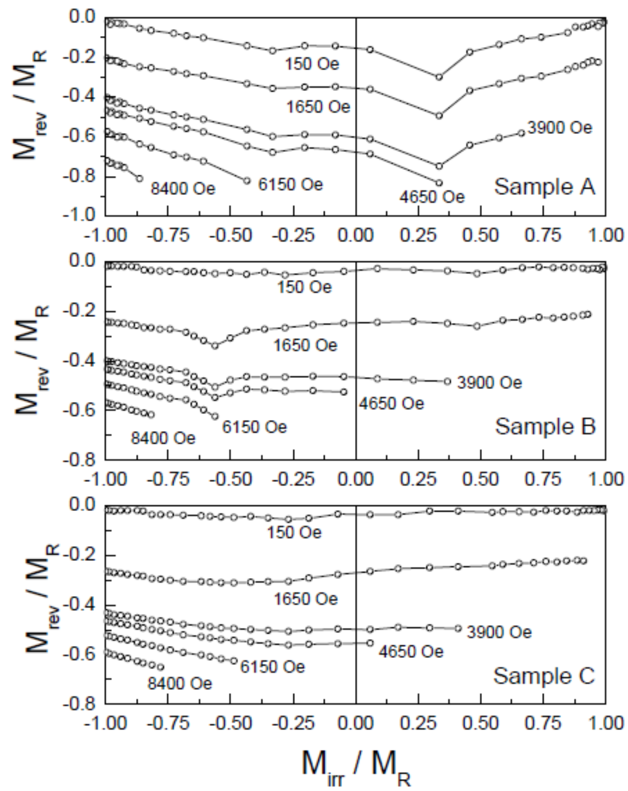

Fig. 4. DCD M_{rev}/M_R component as a function of M_{irr}/M_R at different fixed H_i obtained from the demagnetization curve for each sample.

Acknowledgements

The corresponding author wishes to thank CNPq and CAPES for the partial financial support of this work. D. Bueno and J. Matutes would like to thank the support of Conacyt under the project 32621-U.

References

[1] J. Ormerod, S. Constantinides, J. Appl. Phys. 81 (1997) 4816.

[2] M. Emura, A.C. Neiva, F.P. Missell, K.L. Babcock, J. Ormerod, S. Constantinides, J. Appl. Phys. 83 (1998) 7127.

[3] E.P. Wohlfarth, J. Appl. Phys. 29 (1958) 595.

[4] D.C. Crew, P.G. McCormick, R. Street, J. Appl. Phys. 86 (6) (1999) 3278.

[5] D.C. Crew, L.H. Lewis, J. Appl. Phys. 87 (9) (2000) 4783.

[6] R. Cammarano, P.G. McCormick, R. Street, J. Phys. D: Appl. Phys. 29 (1996) 2327.

[7] D.R. Cornejo, H.R. Bertorello, F.P. Missell, Physica B 320 (2002) 300.

[8] A. Medina-Boudri, D.R. Cornejo, O. Ayala, H.R. Bertorello, J. Matutes-Aquino, J. Magn. Magn. Mater. 254–255 (2003) 219.